

# An intelligent decision-making system for flood monitoring from space

Tanya Vladimirova · Siti Yuhaniz

Published online: 12 November 2009  
© Springer-Verlag 2009

**Abstract** This paper presents the results of a feasibility study on intelligent image processing for flood monitoring on board satellites. The ability to detect temporal changes in images is one of the most important functions in intelligent image processing systems for hazard and disaster monitoring applications. An automatic change detection system is proposed, the purpose of which is to monitor particular areas on earth for flooding events and give warnings to the authorities accordingly. A novel solution to flood detection based on the combined use of optical multispectral imagery and global positioning system reflectometry data is introduced. A fuzzy inference engine is used in the decision-making process, which generates control signals to other subsystems on board the satellite.

**Keywords** Small satellites · Flood monitoring · Multispectral images · Fuzzy inference engine · GPS reflectometry · Database

## Abbreviations

ACCA Automatic cloud cover assessment  
AFRL Air Force Research Laboratory  
AOCS Attitude and orbit control system  
CCD Charge-coupled device  
CHRIS High resolution imaging spectrometer

COTS Commercial-off-the-shelf  
DMC Disaster monitoring constellation  
DSP Digital signal processor  
EO Earth observation  
EO-1 NASA's earth observing one satellite  
ESA European Space Agency  
FPGA Field programmable gate array  
GPS Global positioning system  
HDDR Hard disc data recorder  
HPC-1 High performance computing payload  
LEO Low earth orbit  
MEIS Meteorological earth imaging system  
MSEIS Multi-spectral earth imaging system  
NIR Near-infrared  
PDH Payload data handling system  
PPU Parallel processing unit (X-Sat)  
PPU Payload processing unit (PROBA)  
PROBA Project for on-board autonomy  
SAR Synthetic aperture radar  
SSDR Solid state data recorder  
SSTL Surrey Satellite Technology Ltd

## 1 Introduction

Disaster monitoring from space can provide a powerful tool for advanced warning, assessment of the affected areas and coordination of relief measures. Disaster monitoring requires a quick, almost instantaneous, response which could be achieved if the complete data evaluations were carried out on board. Most earth observation (EO) satellites, such as Landsat, SPOT and IKONOS are large and expensive missions, taking many years to develop.

---

This paper was originally presented at the ECSIS symposium on bio-inspired, learning, and intelligent systems for security (BLISS'07), 9–10 August 2007, Edinburgh, UK.

---

T. Vladimirova (✉) · S. Yuhaniz  
Department of Electronic Engineering, Surrey Space Centre,  
University of Surrey, Guildford GU2 7XH, UK  
e-mail: t.vladimirova@surrey.ac.uk  
URL: <http://personal.ee.surrey.ac.uk/Personal/T.Vladimirova/>

However, small satellites and in particular micro-satellites are emerging that are becoming a better option due to their lower costs, shorter development time and state-of-the-art imaging sensors (Bretschneider et al. 2005). The Surrey Satellite Technology Limited (SSTL), a spin-off company of the University of Surrey and a commercial manufacturer of small satellites have deployed the disaster monitoring constellation (DMC) (Curiel et al. 2003), which at present consists of five micro-satellites in low earth orbit (LEO). DMC provides images to disaster relief agencies worldwide in times of need. The constellation offers a low-cost approach to disaster monitoring based on daily coverage of any place on earth using medium spatial resolution multispectral images.

The ability to detect temporal changes in images is one of the most important functions in intelligent image processing systems for hazard and disaster monitoring applications. Change detection analysis that requires two or more multispectral or synthetic aperture radar (SAR) images acquired over time has recently been adopted in various applications. The NASA's earth observing one (EO-1) spacecraft carries on board several science analysis experiments including cloud detection, flood scene classification and change detection (Chien et al. 2005). In a related project, a specialised processor for on-board change detection is being developed for a repeat-pass change detection and hazards management (Lou et al. 2004). It is predicted that future satellite missions will be capable of carrying out intelligent on-board processing tasks such as image classification, compression and change detection (Zhou and Kaufmann 2002).

Flooding is a devastating disaster that occurs all over the earth. The causes of flooding are heavy rain, hurricanes and undersea earthquakes. Heavy rain is the main factor of flooding, compared to the other two causes. Rain that falls in extended periods causes water from rivers to overflow and flood the nearby areas. Hurricanes destroy dams and levies, which results in heavy flowing of water. Undersea earthquakes can cause big tidal waves such as Tsunami, destroying and flooding coastal areas. The Tsunami disaster on 26 December 2004 (Chen et al. 2005) has led to human tragedy and loss of infrastructure on a very big scale. Processing of downloaded satellite imagery has proven to be effective in monitoring of flooding events. Although envisaged in future missions, performing of flood monitoring on board EO satellites is not yet available due to satellite design limitations and restricted on-board computing resources.

This paper presents the results of a feasibility study on intelligent image processing and decision-making for flood monitoring on board small satellites. An automatic change detection system for flood monitoring missions is proposed (Vladimirova et al. 2006). A novel solution to flood

detection based on the combined use of optical imagery and GPS reflectometry data is introduced. A fuzzy inference engine is employed in the decision-making process, which generates control signals to other subsystems on board the satellite. Multispectral satellite images from SSTL and Landsat satellites as well as Internet are used to evaluate the performance of the investigated algorithms and concepts.

The paper is structured as follows. Section 2 reviews related work on intelligent image processing for use on board satellites. Section 3 introduces the proposed intelligent on-board system and discusses the decision-making block. Section 4 presents evaluation results.

## 2 Image processing on board small satellites

Current commercial EO satellites have very limited image processing capabilities on board. They mostly operate according to a 'store-and-forward' mechanism, where the images are stored on board after being acquired from the sensors and are downlinked when contact with a ground station occurs. The implementation of high performance image processing on board satellites is a challenging task. Many factors have to be considered when deciding on the type of hardware and software to be used on board spacecraft. Intelligent imaging capabilities have already been incorporated in several EO small satellite missions for experimental purposes. For example, small satellites such as UoSAT-5 (Fouquet 1992), BIRD (Haller et al. 2002) and the project for on-board autonomy (PROBA) (Bermyn 2000) are carrying sophisticated experimental imaging payloads. This section briefly reviews advanced imaging payload systems of earth observing small satellites.

The on-board imaging architecture first flown on UoSAT-5 is also implemented on other SSTL small satellite missions. For example, TiungSAT-1, which was launched in 2000, had two earth imaging systems (EIS)—multispectral earth imaging system (MSEIS) and meteorological earth imaging system (MEIS). TiungSAT-1 carried two transputers (T805) as the imaging processors with 20 MHz clocking speed and 4 MB of SRAM. EISs of TiungSAT-1 were capable of autonomous histogram analysis ensuring optimum image quality and dynamic range, image compression, autonomous cloud-editing and high compression thumb-nail image previews. UK-DMC is a satellite of the standard DMC design, with added research and development payloads. Like all of the standard DMC satellites, it carries an optical imaging payload developed by SSTL to provide 32 m ground resolution with an exceptionally wide swath width of over 640 km. The payload uses green, red and near infrared bands equivalent to Landsat TM+ bands 2, 3 and 4. In comparison to the other DMC satellites,

UK-DMC features increased on-board data storage, with 1.5 GB capacity. Images are returned to the SSTL mission operations centre using the Internet Protocol over an 8 Mbps S-band downlink (UK-DMC 2008).

The BIRD satellite that was developed by the German Space Agency is another small satellite with image processing on board. The imaging system of the BIRD satellite is based on two infrared sensors and one charge-coupled device (CCD) camera. A distinctive feature is the specialised hardware unit based on the neural network processor NI1000, which was integrated in the payload data handling system (PDH) of the satellite. PDH is a dedicated computer system responsible for the high-level command distribution and the science data collection between all payloads on the BIRD satellite. The neural network processor implements an image classification system, which can detect fires and hotspots.

The small satellite mission of the European Space Agency (ESA) PROBA has advanced autonomy experiments on-board (Bermyn 2000). The Compact High Resolution Imaging Spectrometer (CHRIS), an EO instrument, demonstrated on-board autonomy with respect to the attitude and orbit control system (AOCS), data handling and resource management. The images from CHRIS are processed in a digital signal processor (DSP) based payload processing unit (PPU) operating at 20 MHz. PPU provides 1.28 Gbit (164 MB) of mass memory and acts as the main processing block for all on-board cameras and other payload sensors.

A significant milestone with respect to on-board intelligent processing is the NASA autonomous “Sciencecraft” concept and the revolutionary TechSat-21 satellite mission of the US Air Force Research Laboratory (AFRL). The TechSat-21 experiment was intended to demonstrate the ability of multiple small satellites flying in formation to perform missions traditionally carried out by single, larger satellites. The Techsat-21 project also included development of on-board science algorithms such as image classification, compression, and change detection (Chien et al. 2002). Under this programme a specialised processor for change detection is developed which is implemented as a multiprocessor system (Lou et al. 2004). The hardware is based on a hybrid architecture that combines field programmable gate arrays (FPGAs) and distributed multiprocessors. Customised FPGA boards and high-speed multiprocessors are being developed because of the limited on-board memory (512 MB or less) and the relatively slow processing speed of the current commercial-off-the-shelf (COTS) components. The required processor performance and memory capacity for the change detection task are estimated as 2.4 GFLOPS and 4.5 GB, respectively. It is aimed that the multiprocessor card will have up to 8 GB on-board memory for the change detection processing task.

FedSat is an Australian scientific small satellite that carries a high performance computing payload (HPC-1). In this mission, a cloud detection system (Williams et al. 2002) and lossless image compression (Dawood et al. 2002) was implemented using reconfigurable computing. Further developments in advanced on-board processing can be seen in the parallel processing Unit (PPU) of X-Sat, a small satellite which is in a process of development at Nanyang Technological University, Singapore. One of the PPU main functions is processing of images acquired from a multispectral camera payload. The processing unit comprises 20 SA1110 StrongArm processors that are inter-linked by FPGAs and clocked at 266 MHz. The increased computational power of PPU is needed for specialised image processing such as real-time compression and unsupervised analysis to optimise the utilisation of the downlink bandwidth (Bretschneider 2003).

Table 1 illustrates the trends in image processing on board small satellites in terms of functionality and summarises computing characteristics of image processing payloads. It can be seen that more on-board image processing functions are included in recent missions. This is made possible due to the availability of more powerful computing resources on board as shown in Table 1.

### 3 An automatic flood monitoring system for use on board satellites

The goal of this research is to implement an intelligent on-board system for flood monitoring using optical images. The flood monitoring process is based on detection of changes between multispectral images taken at different observation times and making decisions based on the identified changes.

So far SAR images have been the choice as remote sensing data for flood detection because of their capability to penetrate clouds which can be quite heavy during flooding events. However, multispectral images have recently risen in importance due to optical EO satellites being relatively cheaper and having better revisit capability than SAR satellites. Multispectral images, taken from DMC satellites, are used to assess the feasibility of the on-board flood monitoring system. DMC images are similar to Landsat TM images in terms of spectral and spatial resolution and are taken in near-Infrared (NIR) (0.76–0.9  $\mu\text{m}$ ), red (0.63–0.69  $\mu\text{m}$ ), and green (0.52–0.62  $\mu\text{m}$ ) spectral bands.

The feasibility study, presented in this paper, is carried out under the following assumptions:

- the EO satellite has a ground repeat track and therefore no geo-rectification is needed;

**Table 1** Functionality trends and computer characteristics of image processing payloads on board small satellites

Launch year	1995	2000	2001	2002	2003	2008 <sup>a</sup>
Satellite	UoSat-5	BIRD	PROBA-1	FedSat	UK-DMC	X-Sat
Ownership	UK	Germany	ESA	Australia	UK	Singapore
Image compression	Yes	Yes	Yes	Yes	No	Yes
Change detection	No	No	No	No	No	Yes
Classification task	Cloud detection	Fire and hotspot detection	Star-pattern recognition	Cloud detection	None	Fire detection
Processor frequency	20 MHz	33 MHz	20 MHz	48 MHz	200 MHz	266 MHz
Hardware parallelism	No	No	No	No	No	Yes
Computing hardware	Transputer	Neural network chip (NI1000)+ DSP	TCS21020 DSP	FPGA	32-bit RISC processor	FPGAs+ multiprocessor system

<sup>a</sup> Cancelled

- the earth areas to be monitored are pre-determined;
- the reference images, which are required for the change detection process, are stored in an on-board image database;
- the sun illumination, atmospheric conditions and other factors affecting the sensed images are the same as the ones of the reference images stored in the on-board database.

### 3.1 System description

The proposed intelligent system for flood monitoring is targeted at the DMC small satellite platform. The decision making process is based on fuzzy logic, which allows the system to deal with the uncertainty and ambiguity of the data input. The block diagram of the proposed system is shown in Fig. 1. The data input of the system is a newly taken image from the optical imagers on board the satellite. The images are split into image tiles of a smaller size for easier processing.

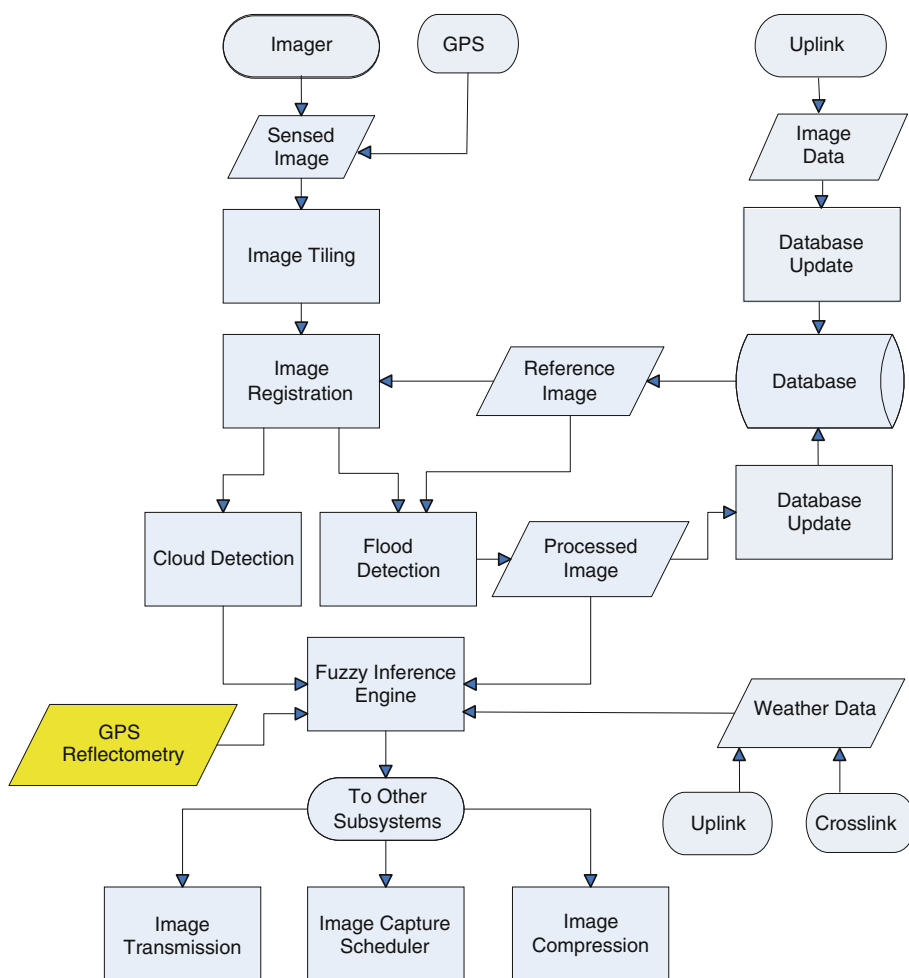
The rectangular boxes in Fig. 1 denote the processing blocks of the system: image tiling, image registration, cloud detection, flood detection, fuzzy inference engine and database update. The parallelogram blocks denote data that flows between the processing blocks, and the cylinder block denotes the on-board database, which stores reference images and processing results. Global positioning system (GPS) data are used to “stamp” the images with the geo-location at the time of capture, providing additional information for the subsequent tasks of image co-registration and identification of the reference image in the database. Bi-statically reflected GPS signals, which are able to penetrate clouds, assist in the water detection process.

Change detection and flood detection are very challenging tasks to be implemented on board small satellites, because they operate on a pair of images: a sensed and a reference image. Image tiling, image registration, and cloud detection are pre-processing blocks that perform additional critical tasks on the input image. Image tiling divides the size of the image into manageable pieces of image data. Image tiling could also be used to make the change detection operation more efficient replacing the direct pixel-to-pixel image comparison by a comparison of statistical features extracted from the individual image tiles.

Image registration is the process of overlaying two or more images of the same scene taken at different times, from different viewpoints, and by different sensors (Zitova and Flusser 2003). The registration process is aimed at finding the optimal spatial and intensity transformations so that the images are aligned. The change detection process is very sensitive to registration errors, especially if it is done on a pixel-by-pixel basis. The effect of image misregistration on the accuracy of remotely sensed change detection is analysed in (Dai and Khorrarn 1998), where it is reported that change detection accuracy drops dramatically within the first pixel of misregistration. Also, an evaluation of the effect of misregistration on moderate resolution satellite imagery concluded that high accuracy of registration is needed in order to achieve a reliable change detection system (Townshend et al. 1992). Several algorithms aimed at the implementation of the image registration pre-processing block in Fig. 1 have been investigated (Yuhaniz et al. 2005a, b), as discussed in Sect. 4 below.

Cloud cover is a problem for multispectral analysis, especially in the tropical regions where the cloud cover is

**Fig. 1** Block diagram of the proposed automatic flood monitoring system



quite heavy. As this research work is focused on using optical images, it is very important to detect clouds in the images before the decision-making process takes place. The automatic cloud cover assessment (ACCA) algorithm used on Landsat 7 is chosen for the cloud detection due to the similarity between the DMC and Landsat images in terms of spectral wavelengths. In addition, ACCA has also been used in several real-time on-board remote sensing experiments (El-Araby et al. 2005; Williams et al. 2002).

“A database is a collection of information that is organised so that it can easily be accessed, managed and updated” [What is Database? TechTarget Website [online]. [http://searchsqlserver.techtarget.com/sDefinition/0,,sid87\\_gci211895,00.html](http://searchsqlserver.techtarget.com/sDefinition/0,,sid87_gci211895,00.html) (Accessed 30 Dec 2008)]. In the context of this system, the database stores images and their associative information. The images stored in the database are the reference images that are being used in the image registration and change detection processing blocks. Other information that is useful for the flood monitoring analysis, for example historical flooding data, could also be stored. The reference image contains the area of interest that is captured by the sensed image. The size of the image

is pre-defined on ground. For example, let the area of interest be in the range of 100 km<sup>2</sup>. The size of the reference image covering 100 km<sup>2</sup> will be 2,500 × 2,500 pixels as the DMC multispectral imager has 32 m ground sampling distance. The image is uploaded with ground control points that will be used to match the sensed image in the image registration processing block.

Databases have not yet been used on board satellites. An on-board hard disc data recorder (HDDR) employing a miniaturised hard drive device could be used to store the database. Hard disc drives are not common on board satellites and are still at an experimental stage. The SSTL’s Beijing-1 DMC satellite carries a pair of HDDRs that have survived launch and the harsh space environment. The HDDRs comprise a 60 GB pressurised hard drive each and are a good candidate for a database implementation. Other than images, the database could include dynamic weather data derived from terrestrial databases, or possibly from meteorological satellites via intersatellite communication. Weather data can be very useful, providing complementary data inputs to the flood detection and cloud detection processing blocks.

The flood detection block is one of the main components of the system. Flood detection and classification using satellite imagery is an active topic of research. Current approaches to this problem can be divided into two categories: change detection based methods and supervised classification based methods. The methods in the first category are widely used in flood detection of satellite imagery. Several flood detection algorithms under this category are investigated (Yuhaniz et al. 2005a, b). The output of this subsystem is a flood map image, which is to be used as an input to the fuzzy inference engine.

Utilizing bistatically reflected GPS signals from LEO for remote sensing on board satellites (Gleason et al. 2005) is a new area of research. GPS reflections are able to penetrate clouds, and also the receivers are cheaper and lighter than traditional SAR imagers. These features are very valuable for the small satellite platform. The potential of GPS reflectometry for water detection (Gleason 2006) is explored in the context of this work. It is proposed that GPS reflectometry signals are used in conjunction with optical images as input data for flood monitoring on board a small satellite. The ability of GPS reflections to penetrate cloud cover will act as a valuable complement and a backup for the flood maps produced by the flood detection processing block.

In this research work, we introduce a fuzzy logic based processing block, called fuzzy inference engine that receives data input from the flood detection processing block. The cloud detection processing block and the GPS reflectometry subsystem also provide input to the decision-making process. The output of the fuzzy inference engine in Fig. 1 is a control signal in the form of a flooding alert of varying strength. This will allow the system to trigger subsequent tasks such as image compression, issuing of a warning alert or scheduling of other imaging operations. For example, if the flooding alert is of high strength, the system would send a high-priority warning alert to the ground station.

### 3.2 Fuzzy inference engine

Fuzzy inference is the process of formulating an associative mapping from given inputs to an output using fuzzy logic. The mapping then provides a basis from which decisions can be made, or patterns discerned (Matlab Fuzzy Logic Toolbox Documentation. <http://www.mathworks.com/access/helpdesk/help/toolbox/fuzzy/index.html?/access/helpdesk/help/toolbox/fuzzy/fp351dup8.html>). Fuzzy associative maps have been used in many applications including computer vision, data classification and automatic control. A fuzzy inference system has three components: fuzzy membership functions, fuzzy operators and if-then rules. A simple example of using fuzzy inference for image classification is given in (Nedeljkovic 2004).

Although the use of fuzzy logic in change detection analysis is an active research area, little work has been done with respect to remote sensing change detection systems. The use of a fuzzy inference system to detect land-cover changes is proposed in (De Souza et al. 2002). The input for the system is a degree of change for each pair of pixels that represent the absolute value of the differences between two images of the same band.

The fuzzy inference engine takes as inputs the flood maps generated by the flood detection processing block as well as additional information from other sources as shown in Fig. 1 and makes decisions which determine the next action of the system.

One of the reasons for using the fuzzy logic approach is to reduce errors during water detection caused by ambiguous data. Fuzzy associative maps employ fuzzy membership functions, instead of crisp data, which provides a better means of dealing with ambiguity. For example the NIR/Red differencing method uses the ratio of the near-infrared and red band images to detect water (Sheng et al. 2001). Image pixels are determined as water if the ratio of near-infrared and red band pixel values is lower than a certain threshold. The threshold that separates water from non-water pixels,  $T_0$ , is located in the valley between two peaks of the histogram of NIR band/red band images as shown in Fig. 2, so a pixel is considered water, if  $\text{NIR/Red} \leq T_0$  or land, if  $\text{NIR/Red} > T_0$ . Often the threshold  $T_0$  is not well defined and this leads to ambiguity in the interpretation of water and non-water pixels. It is expected that the use of fuzzy logic will reduce errors caused by a wrongly defined value of  $T_0$ .

When  $T_0$  is employed as a threshold, some ambiguous pixels would be classified wrongly as water or non-water. However, with the use of fuzzy logic, not only water and non-water pixels but ambiguous pixels can also be considered in the flood detection process. The pixel values can be water, ambiguous or non-water and the membership function will define how close the ambiguous pixels are to either water or non-water pixels. Figure 3 shows the membership function for the image input to the inference engine. The output of the fuzzy inference engine will not

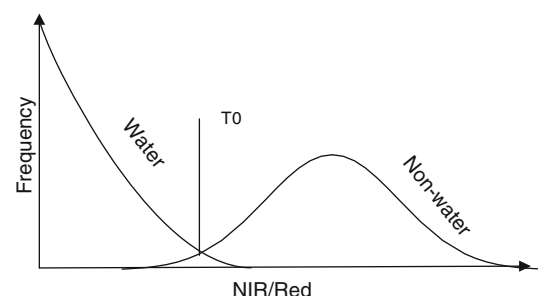
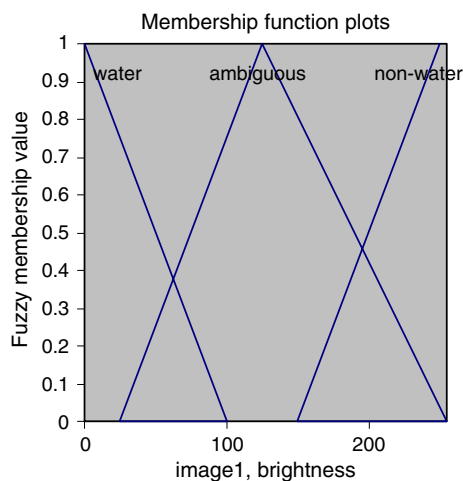
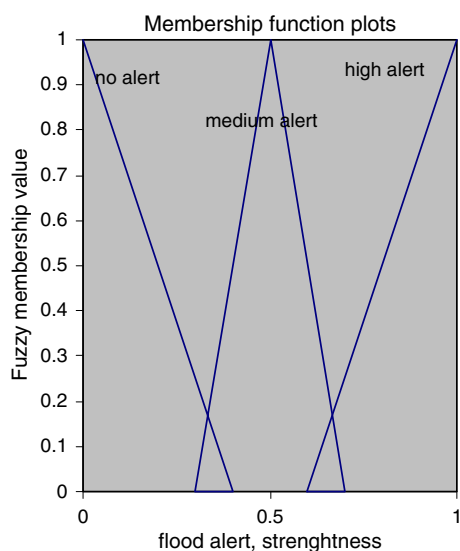


Fig. 2 Histogram of NIR/Red band images





**Fig. 3** Membership function plot of the inference engine input



**Fig. 4** Membership function plot of the inference engine output

be just flooding or not flooding, but it will be expressed in terms of fuzzy sets, for example, “no alert”, “medium-strength alert” and “high-strength alert”, depending on the data input, as shown in Fig. 4.

Different types of imaging data input can be provided to the fuzzy inference engine for the decision making process as detailed in Table 2. The fuzzy inference block can accept pixel values based on the NIR/Red differencing method described above, which is the first choice in Table 2. The second choice of imaging data input for the fuzzy inference is an index for each tile. The index is a certain feature or indicator for each image tile, for example, obtained as a result of classification of the image tiles. Then, the identified features become the input for the fuzzy inference engine. This option has the advantage over the option 1 that it does not use pixel-to-pixel comparison. The

third option is achieved by combining the options 1 and 2 with GPS reflectometry signals that have the ability to penetrate cloud. A transformed image, for example using Fourier Transform, can be used as the imaging input to the fuzzy inference engine too. The last option for the imaging data input to the fuzzy inference engine in Table 2 is the degree of change, which is the absolute value that represents the differences between two images of the same band.

## 4 Experimental results

Extensive numerical experimentation is carried out in order to evaluate and validate different computational solutions for the implementation of the processing blocks in Fig. 1. This section discusses performance evaluation, the use of GPS reflectometry and accuracy assessment results.

### 4.1 Performance evaluation

Software modelling and simulation using Matlab is undertaken to select the optimal image registration and flood detection methods for implementation of the corresponding processing blocks in Fig. 1. The candidate methods are evaluated using multispectral image test sets consisting of a before-flooding reference image and a post-flooding image of the same area. The experimental results presented in this section are derived using the image test set described in Table 3. The post-Tsunami flooding test image of North Sumatra, Indonesia, taken on the 4 January 2005 by the UK-DMC micro-satellite is shown in Fig. 5. The size of the image is  $1,500 \times 2,500$  pixels. The test images are split into image tiles of  $500 \times 500$  pixels before performing flood detection.

One of the objectives of the evaluation is to estimate the execution time and memory capacity required by each of the investigated algorithms for a given image size. The image processing software can be executed in the solid state data recorder (SSDR) unit, part of the imaging payload of the DMC satellite platform. The PowerPC based SSDR unit is used for the performance evaluation presented in this section. The PowerPC processor is capable of executing 280 Dhrystone MIPS at 200 MHz and has 1 MB of RAM. The software was executed on a Pentium M 1.3 GHz personal computer and then the performance was scaled down to match the flight hardware characteristics. The Dhrystone 2.1 benchmark program was run on the Pentium M processor resulting in 1665 Dhrystone MIPS.

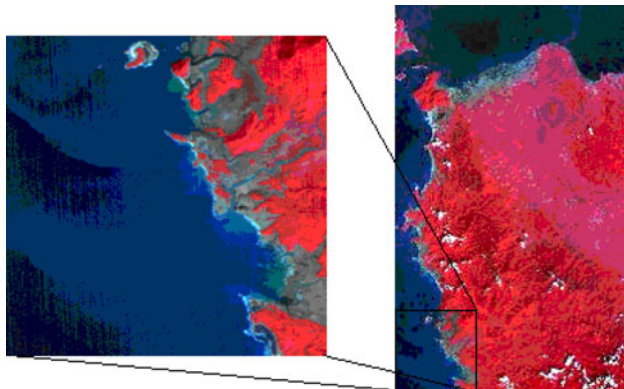
Figures 6 and 7 show the execution times required by the investigated image registration and flood detection methods, respectively. The results are obtained from applying four registration and six flood detection algorithms to a pair of test image tiles of  $500 \times 500$  pixels each

**Table 2** Types of imaging data input for the fuzzy inference engine

<i>N</i>	Input data	Description
1	Pixel value of NIR/Red for image tiles 1 and 2	The rules will determine if each pixel is flooded or not
2	Index for each image tile	An index is calculated for each tile, so no pixel-to-pixel comparison is performed
3	Combination of input 1 and 2 above with GPS reflectometry signals	Same as above with added advantages of immunity to cloud cover
4	Frequency information from the image tiles (e.g. the Fourier Transform of each tile)	An alternative way of image tile processing instead of using spatial information
5	Degree of change	An absolute value that represents the differences between two images of the same band

**Table 3** Test multispectral images used for performance evaluation

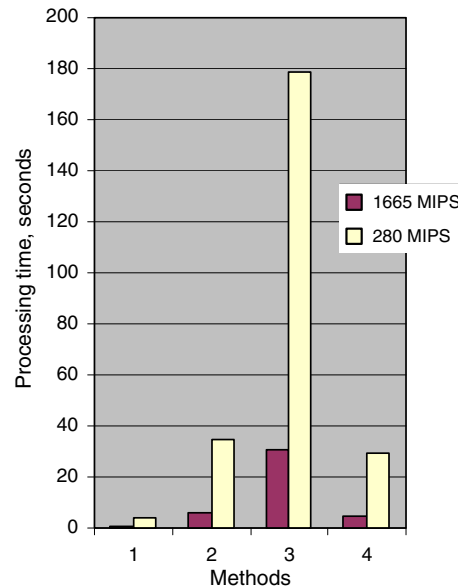
	Date acquired	Source
Before-flooding image		
North Sumatra, Indonesia	15 August 2001	Landsat7 ETM+
After-flooding Image		
North Sumatra, Indonesia	4 January 2005	UK-DMC

**Fig. 5** DMC image of North Sumatra after the Tsunami disaster. The image on the left-hand side is the tile in the bottom left corner of the image on the right (Image courtesy of SSTL)

for the two processors—the test processor (1,665 MIPS) and the targeted processor (280 MIPS).

The tested image registration methods in Fig. 6 are phase correlation, cross correlation, mutual information and Fourier–Mellin registration (Yuhaniz et al. 2005a, b) as follows:

1. *Phase correlation* Phase correlation works by computing the Fourier transform for the input and base image and finding the peaks of their inverse cross power spectrums. It is a fast method, however, it is only useful for registration of images that have translation misalignment.
2. *Cross correlation* Cross correlation is a measure of similarity between pixels on the input and base images, which is used to find the translation shift. It is a slow method, which is sensitive to noise.

**Fig. 6** Estimated processing time of image registration methods. 1 Phase correlation, 2 cross correlation, 3 mutual information and 4 Fourier–Mellin registration

3. *Mutual information* This method is based on probability and information theory. It is a measure of statistical dependency between two data sets and is very useful for registration of multi-modal images.
4. *Fourier–Mellin registration* This method is an extension of the phase correlation algorithm adding the capability to detect rotation and scaling misalignments between the input and base images.

The tested flood detection methods in Fig. 7 are NIR band differencing, NDVI differencing, and four supervised classification methods: parallelepiped, maximum likelihood, minimum distance and Mahalanobis distance (Yuhaniz et al. 2005a, b) as follows:

1. *NIR band differencing* This method subtracts the pixels of the NIR bands of the before and after flooding images, as water in this band has very low reflectance compared to other land cover types. However, this method is very sensitive to factors such as atmospheric



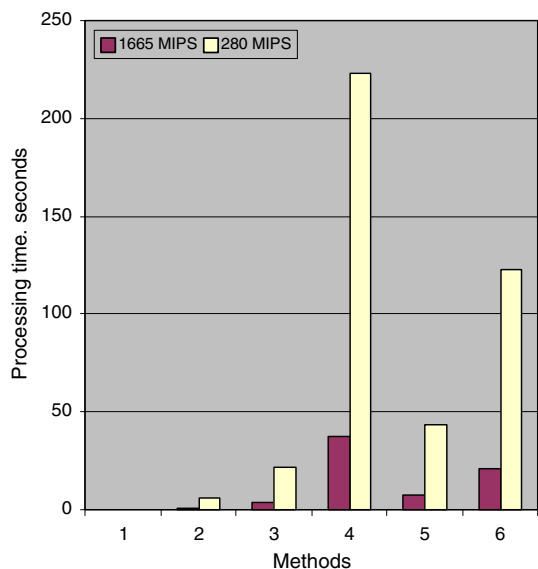


**Fig. 7** Estimated processing time of flood detection methods. 1 NIR differencing, 2 NDVI differencing, 3 parallelepiped, 4 maximum likelihood, 5 minimum distance, and 6 Mahalanobis distance

conditions and sun illumination, which leads to difficulty in setting the threshold that separates water and non-water areas (Nyborg and Sandholt 2001). The calculation of the flooded pixels is expressed as follows:

$$NIR_A - NIR_B \leq T_C \tag{1}$$

where  $NIR_A$  is the after-flooding image in NIR band and  $NIR_B$  is the before-flooding image in NIR.  $T_C$  is the threshold that separates the flooding and non-flooding pixels.  $T_C$  is selected interactively by looking at the  $NIR_A - NIR_B$  histogram.

2. *NDVI differencing* The water pixels are detected based on the normalised difference vegetation index (NDVI). This method has the advantage over NIR differencing of stability to variations of atmospheric conditions, reflection of sun and water turbidity (Nyborg and Sandholt 2001). The calculation of NDVI is expressed as follows:

$$NDVI = (NIR - RED)/(NIR + RED) \tag{2}$$

where RED and NIR stand for the spectral reflectance measurements acquired in the red and near-infrared regions, respectively. The water and non-water pixels are separated by thresholding the NDVI of after and before flooding images, as expressed below:

$$NDVI_A - NDVI_B \leq T_C \quad \text{and} \quad NDVI_A \leq T_W \tag{3}$$

where  $NDVI_A$  is the NDVI for the after-flooding images and  $NDVI_B$  is the NDVI for the before flooding images.  $T_C$  is the threshold that detects the decrease of

NDVI by flood and  $T_W$  is the threshold to exclude non-water surfaces after flood.

3. *Parallelepiped classification* The parallelepiped classifier uses the thresholds of each class signature such as the mean to determine if a given pixel falls within the class or not. The thresholds specify the dimensions (in standard deviation units) of each side of a parallelepiped surrounding the mean of the class in the feature space. If the pixel falls inside the parallelepiped, it is assigned to the class. The parallelepiped classifier is typically used when high speed is required.
4. *Maximum likelihood classification* This method is the most common supervised classifier in the remote sensing application. The water pixels are decided based on the following expression:

$$g_i(x) > g_j(x) \quad \text{for } j \neq i \tag{4}$$

where  $g_i(x)$  is the discriminant function to classify the pixel as water which is expressed as below:

$$g_i(x) = \ln p(x|w_i) + \ln p(w_i) \tag{5}$$

where  $\ln$  is natural logarithm,  $p(x|w_i)$  is the probability distribution of class  $w_i$  (class water) to find  $x$  and  $p_i(w)$  is the probability of class  $w_i$ .

5. *Minimum distance classification* Similar to the maximum likelihood classification, the water pixels are decided based on a discriminant function, but with the following expression:

$$d(x, m_i)^2 > d(x, m_j)^2 \quad \text{for } j \neq i \tag{6}$$

where  $d(x, m_i)^2$  is the discriminant function to classify the pixel as water which is expressed as below:

$$d(x, m_i)^2 = (x - m_i)^t (x - m_i) \tag{7}$$

where  $m$  is the mean of the classes,  $t$  is the transpose of the matrix.

6. *Mahalanobis distance classification* This method decides the pixel as water based on the Eq. 6, with the discriminant function of

$$d(x, m_i)^2 = (x - m_i)^t C^{-1} (x - m_i) \tag{8}$$

where  $C$  is the covariance matrix.

The supervised classification methods (methods 3–6 above) are applied to a pair of images to detect water and then pixel-by-pixel image differencing is performed to find the flooded areas. Figure 8 illustrates a flood map, which is the result of performing flood detection on the test image shown in Fig. 5 using the NIR differencing method. The black areas are the areas affected by flooding.

The SSTL DMC images can have the maximum of 1,200 image tiles of  $500 \times 500$  pixels. Based on the results in Figs. 6 and 7 the minimal total processing time to detect

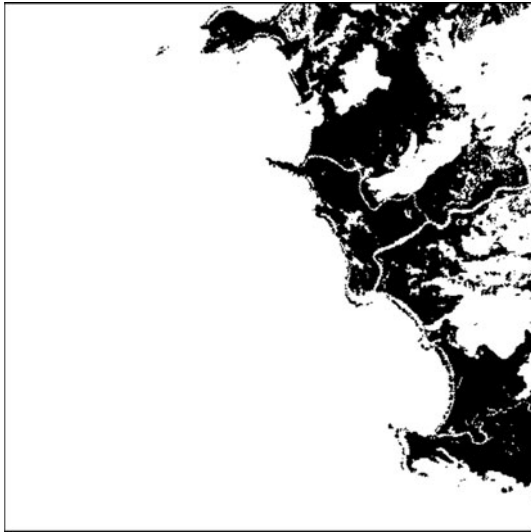
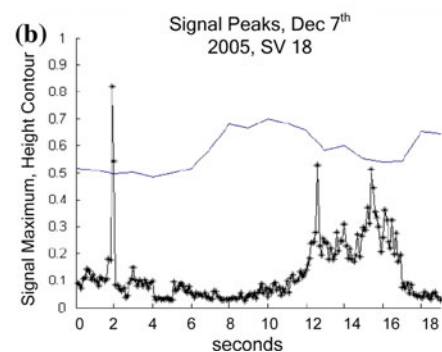
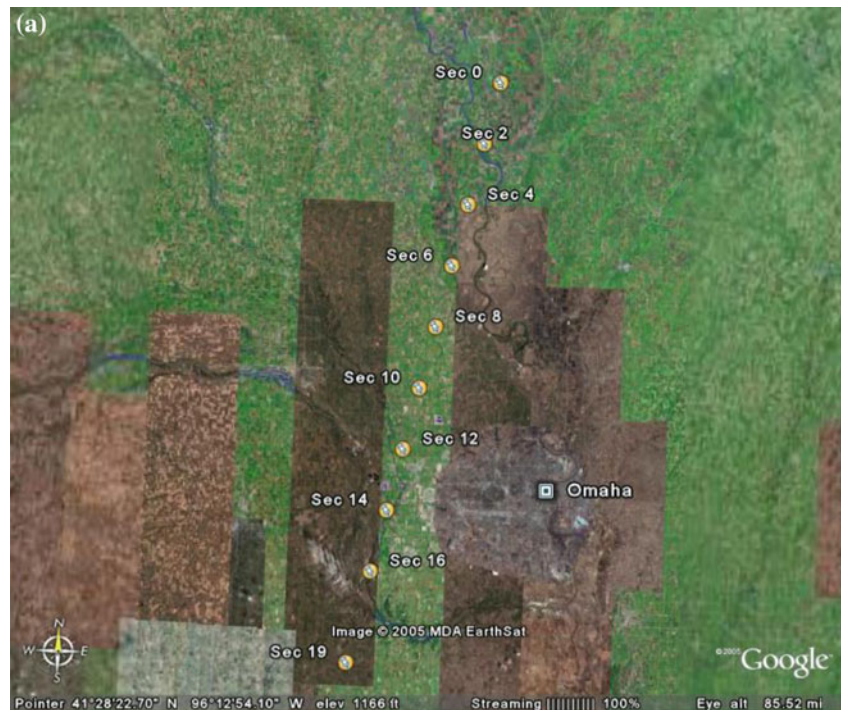


**Fig. 8** The resultant flood detection analysis of North Sumatra, Indonesia, using NIR differencing

**Fig. 9 a** The path of a reflected GPS signal across 19 s of data.  
**b** The peak power returned with estimated height (Image courtesy of GoogleEarth)



flooding for a maximal size image on a PowerPC processor in the DMC SSDR is estimated as 10 h. Such a long processing time is not appropriate for on-board disaster monitoring. This confirms that more powerful computing systems are needed on board EO small satellites. Such a computing system could be realised as a multiprocessor parallel architecture including hardware acceleration of computationally intensive routines on FPGAs.

#### 4.2 Using GPS reflectometry for flood detection

The potential of using GPS reflectometry signals for water detection is illustrated in Fig. 9 (Gleason 2006). As GPS signals travel across the surface they are detectable in LEO using a modified GPS receiver. As the signal traverses the surface it responds to surface features, including near surface water as demonstrated in Fig. 9a. Concerning Fig. 9b, the Missouri river can be seen intersecting the line of reflection points at second 2 (corresponding to the sharp

jump in power) and continuing into Omaha City. The spikes near the 12th and 15th seconds are probably due to the crossings of a loop. It is also probable that the increase in signal power observed over this general region (between seconds 12 and 17), are due to the increased presence of water around the rivers in these areas. However, a more detailed investigation of the ground truth in these areas would be needed before knowing for certain if the increased power levels were due to the presence of surface water.

#### 4.3 Accuracy evaluation of flood detection methods

Here we present experimental results on the accuracy assessment of the flood detection algorithms. One way of measuring the accuracy of water detection is based on the confusion error matrix in Table 4. Omission error (or producer's accuracy) measures the error caused by detecting flooded areas as non-flooded, which result into a missed flooding alert. Commission error (or user's accuracy) measures the error caused by detecting non-flooded areas as flooded, which will generate a false alarm. Overall accuracy measures the accuracy of the flood detection method without taking into account the source of error (errors of omission or commission). Accuracy assessment of flood detection methods is carried out for the North Sumatra test images as described in Table 3. The accuracy results are presented in Table 5, which shows that the NIR/Red differencing method with the fuzzy engine provides

**Table 4** Confusion error matrix

Ground truth/ detection results	Flood	No flood
Flood	Correct detection	False positive (commission error)
No flood	False negative (omission error)	Correct detection

**Table 5** Flood detection accuracy assessment for the image test set of North Sumatra, Indonesia

Method	Commission error (%)	Omission error (%)	Overall accuracy (%)
NIR/Red differencing + fuzzy inference	50	31	92
NIR differencing	52	30	90
NDVI differencing	52	43	90
Parallelepiped	43	59	92
Maximum likelihood	47	62	91
Minimum distance	89	64	68
Mahalanobis distance	64	85	89

the best overall accuracy while keeping the omission errors low.

## 5 Conclusions

This work investigates the feasibility of automatic flood monitoring on board small satellites using optical images. Different from a conventional flood monitoring system, this approach aims to reduce the response time by processing the multispectral images before they are transmitted to the ground station.

A fuzzy inference engine is introduced to support the decision making-process and improve the flood monitoring performance. It is shown that a fuzzy inference engine can help improve water detection by including uncertain data input in the decision-making process.

Several existing image registration and flood detection methods are selected and tested in order to find their expected performance on the computing hardware on board a small satellite. The evaluation results show that high-performance computing and parallel processing are required on board small satellites in order to meet the increased requirements for imaging processing on board remote sensing small satellites.

A novel solution to flood detection is proposed combining GPS reflectometry data and optical images. The ability of GPS reflections to penetrate cloud cover will act as a valuable complement and backup for the flood maps produced from the optical images.

**Acknowledgments** The provision of DMC multispectral satellite images by SSTL and DMCii is gratefully acknowledged. This research is funded by the Government of Malaysia.

## References

- Bermyn J (2000) PROBA—project for on-board autonomy. *Air Space Europe* 2(1):70–76
- Bretschneider T (2003) Singapore's Satellite Mission X-Sat. In: Proceedings of fourth IAA symposium on small satellites for earth observation, Berlin, Germany, 7–11 April
- Bretschneider T, Vladimirova T, Yuhaniz S (2005) Image processing capabilities on board micro-satellites for disaster monitoring. In: Proceedings of second Asian Space Conference, ASC'2005, satellites, applications, socio-economics and regulatory regimes, CDROM, Hanoi, Vietnam, 8–11 November
- Chen P, Liew SC, Kwok LK (2005) Tsunami damage assessment using high resolution satellite imagery: a case study of Aceh, Indonesia. In: Proceedings of IEEE international geoscience and remote sensing symposium, IGARSS'05, vol 2, pp 1405–1408, 25–29 July 2005
- Chien S, Sherwood R, Rabideau G, Castano R, Davies A, Burl M, Knight R, Stough T, Roden J, Zetocha P, Wainwright R, Klupar P, Gaasbeck JV, Cappelaere P, Oswald D (2002) The Techsat-21 Autonomous Space Science Agent. In: Proceedings of first

- international joint conference on autonomous agents and multi-agent systems, part 2, pp 570–577
- Chien S, Sherwood R, Tran D, Cichy B, Rabideau G, Castano R, Davies A, Mandl D, Frye S, Trout B, Shulman S, Boyer D (2005) Using autonomy flight software to improve science return on earth observing one. *J Aerosp Comput Inf Commun* 2:192–216
- Curiel ADS, Boland L, Cooksley J, Bekhti M, Stephens P, Sun W, Sweeting MN (2003) First results from the disaster monitoring constellation (DMC). In: Proceedings of the fourth IAA symposium on small satellites for earth observation, Berlin, Germany, 7–11 April 2003
- Dai X, Khorram S (1998) The effects of image misregistration on the accuracy of remotely sensed change detection. *IEEE Trans Geosci Remote Sens* 36(5):1566–1577
- Dawood AS, Williams JA, Visser SJ (2002) On-board satellite image compression using reconfigurable FPGAs. In: Proceedings of 2002 IEEE international conference on field-programmable technology (FPT), pp 306–310
- De Souza FJ, Velloso MLF, Fonseca OLH (2002) Change-detection of land cover using fuzzy sets and remotely sensed data. In: Proceedings of IEEE international geoscience and remote sensing symposium, IGARSS'02, vol 6, pp 3381–3383
- El-Araby E, Taher M, El-Ghazawi T, Le Moigne J (2005) Prototyping automatic cloud cover assessment (ACCA) algorithm for remote sensing on-board processing on a reconfigurable computer. In: Proceedings of IEEE international conference on field-programmable technology, pp 207–214
- Fouquet M (1992) The UoSAT-5 earth imaging system—in orbit results. In: Proceedings of SPIE conference on small satellite technology and applications, Orlando, Florida, USA, 20–24 April 1992
- Gleason S (2006) Remote sensing of ocean, ice and land surfaces using bistatically scattered GNSS signals from low earth orbit. Ph.D. thesis, University of Surrey, December 2006
- Gleason S, Hodgart S, Sun S, Gommenginger C, Mackin S, Adjrad M, Unwin M (2005) Detection and processing of bistatically reflected GPS signals from low earth orbit for the purpose of ocean remote sensing. *IEEE Trans Geosci Remote Sens* 43(6):1229–1241
- Haller W, BrieB M, Schlicker M, Skrbek W, Venus H (2002) Autonomous onboard classification experiment for the satellite BIRD. In: Proceedings of ISPRS Commission 1 FIEOS conference, vol XXXIV, part 1, 10–15 Nov 2002
- Lou Y, Hensley S, Le C, Moller D (2004) On-board processor for direct distribution of change detection data products. In: Proceedings of IEEE radar conference, pp 33–37, 26–29 April 2004
- Lou Y, Hensley S, Le C, Moller D (2004) On-board processor for direct distribution of change detection data products. In: Proceedings of IEEE Radar conference, pp 33–37
- Nedeljkovic I (2004) Image classification based on fuzzy logic. In: Proceedings of XXth ISPRS congress, vol XXXV. Commission VI, WG VI/1-3, Istanbul. 12–23 July 2004. <http://www.isprs.org/congresses/istanbul2004/comm6/comm6.aspx>. Accessed 30 Dec 2008
- Nyborg L, Sandholt I (2001) NOAA-AVHRR based flood monitoring. In: IEEE international geoscience and remote sensing symposium, IGARSS'01, vol 4, pp 1696–1698
- Sheng Y, Gong P, Xiao Q (2001) Quantitative dynamic flood monitoring with NOAA AVHRR. *Int J Remote Sens* 22(9):1709–1724
- Townshend JRG, Justice CO, Gurney C, McManus J (1992) The impact of misregistration on change detection. *IEEE Trans Geosci Remote Sens* 30(5):1054–1060
- UK-DMC (2008) British National Space Centre DMC Microsatellite, SSTL Website. <http://zenit.sstl.co.uk/index.php?loc=113>. Accessed 30 Dec 2008
- Vladimirova T, Yuhaniz S, Meerman MJ, Stephens P, Hodgson D (2006) Intelligent imaging on board small observation satellites. In: Proceedings of IEEE international geoscience and remote sensing symposium, IGARSS06'06, vol VIII, Denver, Colorado, pp 3939–3942, 31 July–4 Aug 2006
- Williams JA, Dawood AS, Visser SJ (2002) FPGA-based cloud detection for real-time on-board remote sensing. In: Proceedings of IEEE international conference on field-programmable technology, FPT, pp 110–116
- Yuhaniz S, Vladimirova T, Sweeting MN (2005a) Embedded intelligent imaging on-board small satellites. In: Proceedings of Asia–Pacific computer systems architecture conference. Lecture notes in computer science, vol 3740, pp 90–103
- Yuhaniz S, Vladimirova T, Sweeting MN (2005b) Flood detection of Tsunami affected areas using multispectral images. In: Proceeding of the 26th Asian conference of remote sensing, Hanoi, Vietnam, 7–11 November
- Zhou G, Kaufmann P (2002) On-board geo-database management in future earth observing satellites. In: Proceedings of at the global, regional and local scale mid-term symposium on integrated remote sensing in conjunction with Pecora 15/Land Satellite Information IV Conference, Denver, USA, 10–15 November 2002
- Zitova B, Flusser J (2003) Image registration methods: a survey. *Image Vis Comput* 21(11):977–1000